The 2010 IEEE/RSJ International Conference on
Intelligent Robots and Systems
October 18-22, 2010, Taipei, Taiwan

Limit Cycle Based Walk of a Powered 7DOF 3D Biped with Flat Feet

Yuzuru Harada†, Jun Takahashi†, Dragomir Nenchev* and Daisuke Sato*

Abstract— **Our ultimate goal is introducing energy-efficient walking patterns to actual humanoid robots. It is known that limit cycle based walking methods, e.g. Passive Dynamic Walking, have such a desired property. Unfortunately, the application of the methods has been limited to simple planar biped models. In this paper, we propose a way of extending limit cycle based walking pattern generation toward a 7DOF 3D biped with ankles, knees, an upper body and with flat feet. This is achieved via first decoupling roll and pitch motions in the frontal/sagittal planes, and then, by designing a limit cycle based walking pattern in the sagittal plane for a planar 5DOF model with ankles, knees and torso. Robustness of the motion is ensured via a feedback control method based on mechanical energy. Then, the planar motion pattern is projected back into 3D space by incorporating dynamic components for gravity compensation and designing a proper trajectory for ankle roll motion. The performances of the walking pattern generator and the controller are confirmed via numerical simulations. The results are presented also as animated motion of a 7DOF 3D biped in the accompanying video.**

I. INTRODUCTION

In the near future, humanoid robots are expected to work in our everyday life environment. At present, however, they have quite limited capabilities, such as imperfect walking or running, balance control excluding the presence of external forces, simple recognition and communication capabilities. Therefore, the field of application of humanoid robots is limited now to research, education and entertainment [1].

One of the problems to be solved is how to improve walking pattern generation and walking control. It should be apparent that nowadays humanoid robots walk in an unnatural way with bended knees, which also leads to inefficiency in terms of energy requirement and mechanical power consumption. This is due to widely adopted walking pattern generation based on simplified dynamical models, e.g. linear inverted pendulum [2] or carted inverted pendulum [3]. These methods, also known as "Zero-Moment Point (ZMP)" methods, make use of the inverse kinematics to manipulate the ZMP or the center of mass (CoM) position and velocities. A singularity occurs thereby at the straight-knee configuration and consequently, it becomes impossible for the biped to take a stance with straighten knees. This problem is related to energy efficiency because a bended-knee stance consumes more energy than a straight-knee one [4]. Several research works have already attempted to address this problem in various ways [5]–[8].

The authors are with the Department of Mechanical Systems Engineering, Faculty of Engineering, Tokyo City University, 1-28-1, Tamazutsumi, Setagaya-ku, Tokyo 158-8557, Japan.
† {harada,takahashi}@rls.mse.tcu.ac.jp
* {nenchev,dsato}@tcu.ac.jp

One possible way to solve the above problem is walking pattern generation derived from studies on human walking [9]. These studies lead to the "Passive Dynamic Walking (PDW)" concept proposed by McGeer [10]. He clarified the mechanism of steady walking of a simple planar biped on an inclined surface under gravity and without any additional force inputs. This can be regarded as an ultimate walking pattern generation method from the viewpoint of energy efficiency [11]. Many studies have addressed PDW since, shedding light on the complexity of the problem. This complexity is the reason why most of the studies deal with very simple planar cases such as single-joint (hip) compass type bipeds [12] or two-joint (hip and knee) ones [13].

PDW studies with 3D biped models, on the other hand, are still quite rare. The reason is that the limit cycle that ensures periodic and stable motion for compass bipeds [12], may cease to exist. McGeer, for example, tried to model 3D PDW incorporating both roll and yaw rotation in the ankles [14]. He found that the walking pattern cannot be stabilized because of roll-to-pitch and/or yaw-to-pitch couplings that inhibit the generation of a stable limit cycle. The important role of these couplings becomes also apparent from the work [15]. On the other hand, we should note that there are passive 3D biped mechanisms that can walk down a slope. Such mechanisms are equipped with feet of curved shape to remedy the roll-to-pitch coupling, and also with arm-like links that help in solving the yaw-to-pitch coupling problem [16], [17].

Powered 3D bipeds have been also considered because they can walk on a flat surface. One way for ensuring energy efficiency is preserving passivity as much as possible. This can be done by decoupling the sagittal from the frontal plane motions and stabilizing roll motion in the frontal plane via direct or indirect power sources, as shown by Kuo [18]. Another way for ensuring power efficiency is by involving optimization methods that also guarantee a periodic walking pattern [19]. A recent work shows that the efficiency of limit cycle based walking can be exploited in 3D with a proper control that considers coupling and yaw steering [20].

At present, it is not known whether energy efficient methods like those mentioned above can be applied to humanoid robots. There are numerous hurdles to overcome. One of them is related to the foot shape. Note that the powered 3D bipeds above have special feet: curved in the case of Kuo [18], or point feet in the case of optimization-based methods [19] and yaw steering [20]. Works on powered 3D limit cycle based bipeds with flat feet, on the other hand, are non existent. We focus on flat feet in this work because most existing humanoid robots have such feet. Another challenge

can be related to the hybrid dynamics nature of PDW: the roles of stance and swing leg are exchanged instantaneously during completely inelastic impacts between the swing leg and the ground. Mass distribution plays also a very important role [10], [21], and hence can be a great challenge, as can be speed control, yaw steering, walking on uneven terrain etc.

In this work, we make an attempt to come closer to the goal of applying a PDW-like generation method to a 3D biped model resembling a present humanoid robot in the sense of having a relatively large number of powered joints, flat feet and suitable mass distribution, e.g. with relatively heavy torso and feet. We also propose an appropriate control law and show via numerical simulations that the model is capable of energy-efficient stable cyclic walking with robustness.

The papers is organized as follows. First, we present the background and the assumptions in Section II. Next, we introduce our 3D biped model in Section III. We describe the controller design in Section IV. Then, we present the results of numerical simulations in Section V. Finally, the conclusions are given in Section VI.

II. BACKGROUND AND ASSUMPTIONS

The basis of the method discussed here is the same as in our previous work where limit cycle based motion of the simplest possible 3D biped with flat feet, ankle roll and pitch joints and a hip pitch joint was addressed [22].

An nDOF biped is modeled as a hybrid dynamical system with two phases: single support phase and leg switch phase. The equation of motion describing the single support phase is given as:

$$\boldsymbol{M}(\boldsymbol{q})\ddot{\boldsymbol{q}} + \boldsymbol{C}(\boldsymbol{q},\dot{\boldsymbol{q}})\dot{\boldsymbol{q}} + \boldsymbol{g}(\boldsymbol{q}) = \boldsymbol{\tau}, \tag{1}$$

where $\boldsymbol{M}(\boldsymbol{q}) \in \Re^{n\times n}$ denotes the body inertia matrix, $\boldsymbol{C}(\boldsymbol{q},\dot{\boldsymbol{q}}) \in \Re^{n\times n}$ is the Coriolis and centrifugal forces matrix, $\boldsymbol{g}(\boldsymbol{q}) \in \Re^{n}$ is the gravity term and $\boldsymbol{\tau} \in \Re^{n}$ is the control torque. The leg switch phase, on the other hand, occurs instantaneously when the foot of the swing leg collides with the ground. As usual in PDW studies, it is assumed that the collision is a completely inelastic one. Hence, the impact dynamics is modeled after the principle of conservation of angular momentum, as follows:

$$\boldsymbol{Q}^{-}(\boldsymbol{q}^{-})\dot{\boldsymbol{q}}^{-} = \boldsymbol{Q}^{+}(\boldsymbol{q}^{+})\dot{\boldsymbol{q}}^{+} - \boldsymbol{J}_C^T\boldsymbol{\eta}_C, \tag{2}$$

where superscripts $(\circ)^-$ and $(\circ)^+$ denote pre- and post-collision values, respectively, $\boldsymbol{Q}^{-}(\boldsymbol{q}^{-})\dot{\boldsymbol{q}}^{-}$ denotes the angular momentum at pre-collision and $\boldsymbol{Q}^{+}(\boldsymbol{q}^{+})\dot{\boldsymbol{q}}^{+}$ denotes the angular momentum at post-collision, and $\boldsymbol{Q}^{-}(\boldsymbol{q}^{-}) \in \Re^{n\times n}$ and $\boldsymbol{Q}^{+}(\boldsymbol{q}^{+}) \in \Re^{n\times n}$ have the meaning of inertia matrices. $\boldsymbol{J}_C^T\boldsymbol{\eta}_C$ is the constraint momentum vector for the locking of specified joints. e.g. hip and knee joints.

Further assumptions made in the prior work were that the robot moves on a flat ground straightforward (no yaw steering), the stance leg being always fixed to the ground (no slip), and the feet being always parallel to the ground.

To ensure a PDW-like walking of our 3DOF 3D biped under these assumptions, we employed a composite control law comprising the following five components:

- decoupling control for motions in the sagittal and frontal planes;
- control component for reconstructing the gravity environment in the sagittal plane;
- energy control with gravity-like feedforward component to drive the motion and a feedback component for asymptotic stabilization to a passive-like limit cycle in the sagittal plane;
- control component for synchronizing motions in the sagittal and frontal planes via a simple hip lock mechanism;
- path planning and PD control for roll motion in the frontal plane.

We would like to focus on two of these components. First, consider the energy control component. It was originally proposed in [23], for the simplest compass type biped with two driven joints (ankle and hip). It can be represented in a general form covering 2D bipeds of an arbitrary number of DOF:

$$\boldsymbol{\tau}_e = \boldsymbol{\mu}\frac{m_{tot}g\dot{r}_{Cx}\tan\phi - k_e(E - E_d(r_{Cx}))}{\boldsymbol{\mu}^T\dot{\boldsymbol{q}}}, \tag{3}$$

where $m_{tot}g\dot{r}_{Cx}\tan\phi$ denotes the "virtual gravity" feedforward component that drives the model, ϕ standing for the slope angle of a "virtual slope", m_{tot} is the total mass of the model, g is the gravity acceleration and r_{Cx} is the horizontal CoM position. The other component on the r.h.s. is the energy feedback component, with E and E_d denoting the current and the reference mechanical energy, k_e being the feedback gain. $\dot{\boldsymbol{q}}$ is the joint velocity vector, while $\boldsymbol{\mu}$ denotes the torque ratio. For the simplest compass type biped with two driven joints (ankle and hip), which is a planar projection of our 3DOF 3D biped, $\boldsymbol{\mu} = \begin{bmatrix}\mu & 1\end{bmatrix}^T$. It should be emphasized that with this control law, the control torque curves become *almost* constant, which can be considered to be an important indicator of energy efficiency, as noticed in [23]. Based on this observation, a constant torque ratio μ for the two joints was considered to be the most appropriate.

Next, consider the roll motion component. Because of the decoupling, it is possible to assign an arbitrary path. We tried two approaches; one based on a spline for smooth roll motion, the other on empirical observation of coupling between the CoM motion components. The empirical approach clearly lead to better results in terms of energy efficiency [22].

In this work, we adopt the same assumptions as above. In addition, we will assume here that the knee joint of the stance leg is locked in the straightened position during the entire cycle and that the upper body stays always parallel to the vertical. As far as the motion in the swing leg knee joint is concerned, we will explore two possibilities hereafter. Similar control components will also be considered. An important problem to be solved below is how to determine the torque ratio in case of a multi-DOF system as ours.

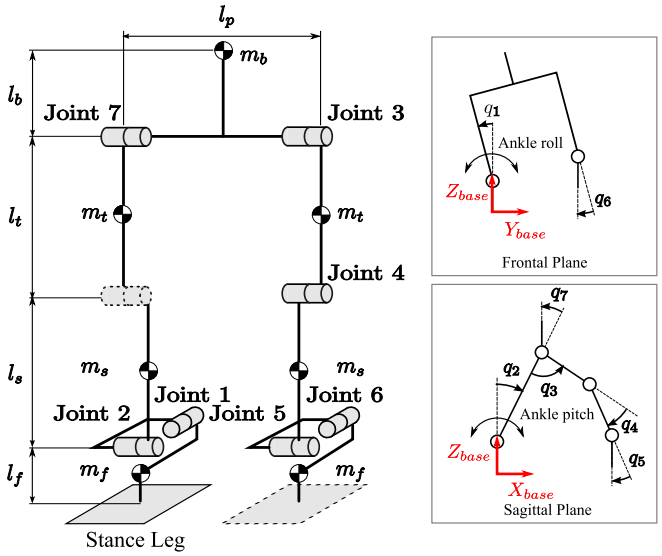

Fig. 1. 7DOF 3D biped model: (a) kinematic structure, (b) generalized coordinates of the model.

TABLE I

PHYSICAL PARAMETERS OF THE 7DOF 3D BIPED MODEL.

Link name	Mass [kg]	Length [m]
Upper body/Pelvis	$m_b = 10.0$	$l_b = 0.5$ / $l_p = 0.3$
Thigh	$m_t = 2.5$	$l_t = 0.5$
Shank	$m_s = 2.5$	$l_s = 0.5$
Foot	$m_f = 1.0$	$l_f = 0.2$

III. 3D BIPED MODEL

This paper deals with a 7DOF 3D biped model as shown in Fig. 1. The model is composed of seven joints and seven links, including two legs and a torso. Each leg consists of a foot, a shank and a thigh. The seven joints are the ankle joints with 2DOF each (Joints 1,2,5 and 6), the 1DOF hip joint (Joint 3), the knee joint of the swing leg (Joint 4)[1] and the 1DOF torso joint (Joint 7). The physical parameters of the biped model are shown in Table I. The CoM positions of the leg/feet bodies are located in the middle of the respective link. Link moments of inertia and friction in the joints will be ignored. The generalized coordinates are the joint angles $q_i, i = 1, 2, ..., 7$, whereas the generalized forces at the joints will be denoted as $\tau_i, i = 1, 2, ..., 7$.

IV. CONTROLLER

As mentioned in the Introduction, while there are numerous works on limit cycle based simple 2D bipeds, there are non on limit cycle based 3D bipeds, mainly because the coupling between motions in the sagittal and frontal planes are not well understood yet. A commonly used approach, adapted also here, is to decouple first these motions via control, and then to generate a limit cycle based walking pattern for the respective sagittal plane model.

[1]During the single support phase, the knee joint of the stance leg is locked.

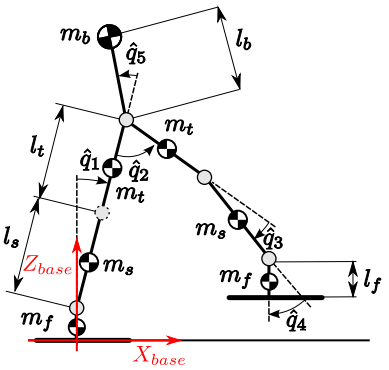

Fig. 2. Virtual 2D model.

A. Decoupling control

Decoupling can be done in a straightforward manner via the equation of motion (1), and more specifically, via the components of matrices $\boldsymbol{M}(\boldsymbol{q})$ and $\boldsymbol{C}(\boldsymbol{q}, \dot{\boldsymbol{q}})$. For our 7DOF model, these are 7×7 matrices. The second to the fifth and the seventh rows of the equation of motion describe the moments on the pitch joints (Joints 2, 3, 4, 5, 7). The first and the sixth columns of these two matrices describe the coupling moment due to the roll joint motions (Joints 1 and 6). Therefore, the matrices for decoupling control become:

$$\boldsymbol{M}^*(\boldsymbol{q}) = \begin{bmatrix} 0 & M_{12} & M_{13} & M_{14} & M_{15} & 0 & M_{17} \\ M_{21} & 0 & \cdots & \cdots & 0 & M_{26} & 0 \\ M_{31} & \vdots & \ddots & & \vdots & M_{36} & \vdots \\ M_{41} & \vdots & & \ddots & \vdots & M_{46} & \vdots \\ M_{51} & 0 & \cdots & \cdots & 0 & M_{56} & 0 \\ 0 & M_{62} & M_{63} & M_{64} & M_{65} & 0 & M_{67} \\ M_{71} & 0 & \cdots & \cdots & 0 & M_{76} & 0 \end{bmatrix}, \quad (4)$$

$$\boldsymbol{C}^*(\boldsymbol{q}, \dot{\boldsymbol{q}}) = \begin{bmatrix} 0 & C_{12} & C_{13} & C_{14} & C_{15} & 0 & C_{17} \\ C_{21} & 0 & \cdots & \cdots & 0 & C_{26} & 0 \\ C_{31} & \vdots & \ddots & & \vdots & C_{36} & \vdots \\ C_{41} & \vdots & & \ddots & \vdots & C_{46} & \vdots \\ C_{51} & 0 & \cdots & \cdots & 0 & C_{56} & 0 \\ 0 & C_{62} & C_{63} & C_{64} & C_{65} & 0 & C_{67} \\ C_{71} & 0 & \cdots & \cdots & 0 & C_{76} & 0 \end{bmatrix}. \quad (5)$$

Then, the decoupling control torque component can be written as:

$$\boldsymbol{\tau}_{dcp} = \boldsymbol{M}^*(\boldsymbol{q})\ddot{\boldsymbol{q}}^* + \boldsymbol{C}^*(\boldsymbol{q}, \dot{\boldsymbol{q}})\dot{\boldsymbol{q}}, \quad (6)$$

where $\ddot{\boldsymbol{q}}^*$ denotes the joint acceleration vector of the previous sampling time.

B. Limit cycle based control in the sagittal plane

Once decoupling is ensured, we can focus on the control of the respective 2D model in the sagittal plane. This model, shown in Fig. 2, will be called "virtual 2D model." The

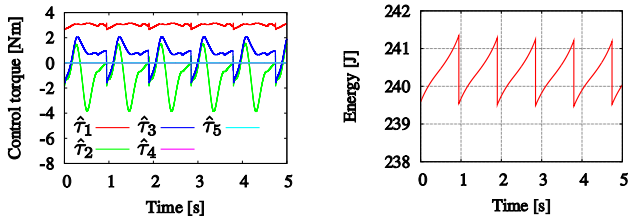

(a) (b)

Fig. 3. PDW of the virtual 2D model with PID control of the knee joint with cubic sine reference trajectory and virtual slope angle $\phi = 0.02$ rad.

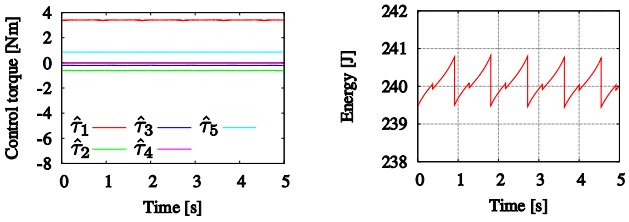

(a) (b)

Fig. 4. PDW of the virtual 2D model with passive knee joint plus knee lock control and virtual slope angle $\phi = 0.017$ rad.

generalized coordinates of the model are the five joint angles $\hat{q}_i, i = 1, 2, ..., 5$. Further on, the relation between the generalized coordinate vectors of the 3D model and the virtual 2D model, $\boldsymbol{q}$ and $\hat{\boldsymbol{q}}$, respectively is:

$$\begin{aligned} \hat{\boldsymbol{q}} &= \boldsymbol{S}\boldsymbol{q} \\ \boldsymbol{S} &= \begin{bmatrix} 0 & 1 & 0 & 0 & 0 & 0 & 0 \\ 0 & 0 & 1 & 0 & 0 & 0 & 0 \\ 0 & 0 & 0 & 1 & 0 & 0 & 0 \\ 0 & 0 & 0 & 0 & 1 & 0 & 0 \\ 0 & 0 & 0 & 0 & 0 & 0 & 1 \end{bmatrix}. \end{aligned} \tag{7}$$

To ensure a PDW-like motion for the virtual 2D model, we adopt the control law (3). Originally, this energy feedback control law was applied to the simplest compass biped model with two driven joints in the ankle and the hip [23]. Note that for such a biped it is easy to determine the torque ratio vector $\boldsymbol{\mu}$, since it contains just one unknown scalar. It was also therefore straightforward to apply the control to the simple 3DOF 3D model in our previous work [22]. In this work, however, our virtual 2D model has five actuated joints. The torque cannot be therefore distributed between the joints in an unique way.

To solve the torque distribution problem, we took a trial-and-error approach regarding the torque in the knee joint ($\hat{\tau}_3$). Recall that our motion strategy is such that torques in the ankle pitch joint ($\hat{\tau}_4$) and the torso joint ($\hat{\tau}_5$) are predetermined since the foot and the torso are always parallel and orthogonal to the ground, respectively. Indeed, these torques can be derived via the Lagrange multiplier method, using the constraint equation:

$$\begin{aligned} \hat{\boldsymbol{J}}_M \dot{\hat{\boldsymbol{q}}} &= \boldsymbol{0}, \\ \hat{\boldsymbol{J}}_M &= \begin{bmatrix} 1 & 0 & 0 & 0 & 1 \\ 1 & 1 & 1 & 1 & 0 \end{bmatrix}. \end{aligned} \tag{8}$$

The first method used to derive the torque in the knee joint was PID control with a reference trajectory generated via a cubic sine function [13]. Figure 3 shows torque and mechanical energy data graphs from a simulation with our virtual 2D biped. It is seen that the biped's walking is cyclic and stable, with appropriate energy shaping. But it also becomes apparent that there are large fluctuations in the knee and hip torques, which is a clear indicator of lack of efficiency.

The second approach we took was to leave the knee joint unactuated, until the swing leg is fully extended passively. Thereafter, the knee joint was kept locked until the start of the leg exchange phase. Simulation data are shown in Fig. 4. Periodic and stable walking can be confirmed from the mechanical energy graph. When compared to the energy graph from the previous approach (Fig. 3 (b)), it is seen that the amplitude of the energy is smaller, which means that less mechanical work will be needed to recover the energy loss due to foot impacts. Note also that around the mid point of each cycle, small energy jumps are seen. These are due to energy loss in the impacting knee joint. But the mechanical work needed for recovering these losses is quite small.

Further on, an important result becomes apparent from the torque graphs: all torques are *almost* constant, which indicates a highly efficient performance. From this result, a suitable torque ratio vector $\boldsymbol{\mu}$ to be used in control law (3) can be derived. The only thing left to be done then is energy shaping. The desired energy function $E_d(r_{Cx})$ is designed as:

$$E_d(r_{Cx}) = m_{tot} g r_{Cx} \tan\phi + E_0 + E_{loss}, \tag{9}$$

where E_0 is the initial mechanical energy, E_{loss} denotes energy loss due to knee joint impacts. Before locking the knee joint, E_{loss} is zero, thereafter it can be calculated as $E_{loss} = E^+ - E^-$, where E^- and E^+ denote pre- and post-impact mechanical energy, respectively. Note that although small, the knee joint loss of energy influences stability. Therefore, we had to include the term in the energy shaping.

We performed two simulations to confirm the efficiency and robustness of the energy feedback control law. The parameters used therein are: virtual slope angle $\phi = 0.013$ rad, $\boldsymbol{\mu} = \begin{bmatrix} 1 & -0.18 & -0.06 & 0 & 0.25 \end{bmatrix}^T$, $k_e = 10$ s^{-1} and $E_0 = 240$ J. With the first simulation, we confirm robustness when motion starts from within the neighborhood of the stable equilibrium state. Figure 5 shows the results in terms of joint torque and phase portrait. It can be seen that the states of the biped model converge asymptotically to a stable limit cycle. Thus, we can confirm the important result that with the proposed control law, deviations from the initial conditions can be tolerated.

Next, we performed a simulation with uncertainty due to a 10% deviation in the nominal mass parameters. Motion starts with the exact initial conditions. The results are shown in Fig. 6. From the phase portrait it should be apparent that the proposed energy feedback control stabilizes the walking pattern despite model errors. When compared with

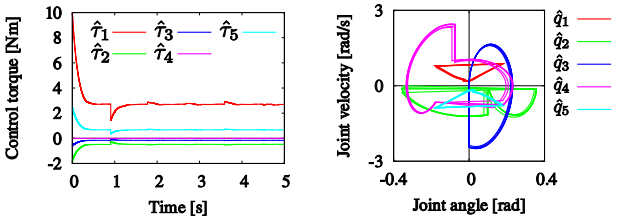

(a) (b)

Fig. 5. Limit cycle based walking with the virtual 2D model (perfect dynamic model) using energy feedback control. Motion starts from the neighborhood of the stable equilibrium point: (a) control torque vs. time, (b) phase portrait.

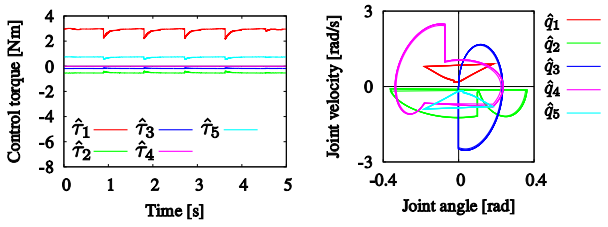

(a) (b)

Fig. 6. Limit cycle based walking with the virtual 2D model (imperfect dynamic model) using energy feedback control. Motion starts at the stable equilibrium point: (a) control torque vs. time, (b) phase portrait.

the previous simulations, however, we can see joint torque jumps during the leg switch phase. The reason is that because of the parameter errors, the control law leads initially to convergence to a state trajectory which differs from the stable limit cycle in the single support phase. The torque jumps increase when the masses deviate further from the nominal values. The stability of the walking pattern, however, can be maintained within a relatively large range.

C. Application to the 3D model

In order to apply the above results to the 3D model, we have to solve three more problems. First, a transformation to 3D is needed. This can be ensured via the following relation:

$$\boldsymbol{\tau}_{e3D} = \boldsymbol{S}^T \boldsymbol{\tau}_e, \tag{10}$$

where $\boldsymbol{S}$ is the same as in (7). Second, we have to reconstruct the gravity environment for the virtual 2D model, in order to eliminate the influence of the roll motion in the frontal plane. This can be done with the following torque component (see also [22]):

$$\boldsymbol{\tau}_g = \boldsymbol{g}(\boldsymbol{q}) - \hat{\boldsymbol{g}}(\hat{\boldsymbol{q}}), \tag{11}$$

where $\hat{\boldsymbol{g}}(\hat{\boldsymbol{q}})$ denotes the gravity torque of the virtual 2D model.

Third, the motion in the ankle roll joint has to be specified. Since motion control in the frontal plane is decoupled from that in the sagittal plane, basically, we can assign an arbitrary trajectory to that joint. It is not clear, though, how to ensure energy efficiency thereby. So, we take again an empirical approach based on the experience in our previous work [22]. In simple terms, we did the following:

1) we repeated the simulation with reasonable flat torque of the ankle roll joint a number of times;
2) we checked the input torque, mechanical energy, angular momentum and the trajectory of the CoM;
3) we generated a reference trajectory of the joint angle based on the best results in the simulations. Note that we defined the best results from the trajectory with the smallest joint torque.

Finally, the composite control torque containing all components necessary to ensure stable walking generation based on a limit cycle for our 7DOF 3D biped, can be expressed as:

$$\boldsymbol{\tau} = \boldsymbol{\tau}_{dcp} + \boldsymbol{\tau}_{e3D} + \boldsymbol{\tau}_g + \boldsymbol{\tau}_{roll} + \boldsymbol{J}_M^T \boldsymbol{\lambda}_C, \tag{12}$$

where $\boldsymbol{\tau}_{roll}$ denotes the control torque for stabilization of the motion in the frontal plane and $\boldsymbol{J}_M^T \boldsymbol{\lambda}_C$ denotes the torque for the constraints. The constraints include the hip locking torque for synchronization between the motions in the frontal and sagittal planes [22], the locking torque of the knee joint of the swing leg, and the control torque of the ankle joint of the swing leg and the upper body.

V. NUMERICAL SIMULATIONS OF LIMIT CYCLE BASED WALKING OF A 7DOF 3D BIPED

We perform two simulations with our 3D biped to compare the performance with two different trajectories for the ankle roll motion. The first simulation uses a spline trajectory for roll, the second one — the empirically obtained trajectory described above. The results are shown in Fig. 7, whereas $\phi = 0.013$ rad and $E_0 = 240$ J. We used a variable energy feedback gain: $k_e = 100t$ s^{-1}, t denoting time. This feedback gain was set to avoid excessive joint torque due to the collision between the foot and the floor during the leg switch phase. Also, time t is reset at the collision instant between the foot and the ground.

Figures 7 (a) and (b) show the phase portraits. It becomes apparent that the biped model can walk periodically indeed. On the other hand, from Figs. 7 (c) and (d), we can understand that the maximum control torque in the roll joint is smaller with the empirical reference trajectory than that with the spline reference trajectory. To compare the energy efficiency, we use dimensionless specific mechanical cost of transport, defined as [11]:

$$c_{mt} = \frac{(\text{energy used})}{(\text{weight}) \cdot (\text{distance traveled})}. \tag{13}$$

Biped walking with roll spline has $c_{mt} \approx 0.95$, while that with the empirical method has $c_{mt} \approx 0.85$. Note that Honda humanoid ASIMO has been evaluated to have $c_{mt} \approx 1.6$ [11].

Further on, since our biped is equipped with flat feet, we have to also check the ZMP trajectory. Figures 7 (e) and (f) show the ZMP position and the center of the foot of the stance leg. It can be seen that in the first simulation, the oscillation of the ZMP position is larger than that in the second simulation. Hence, we can conclude that it is possible to design a robot with smaller feet when using the control

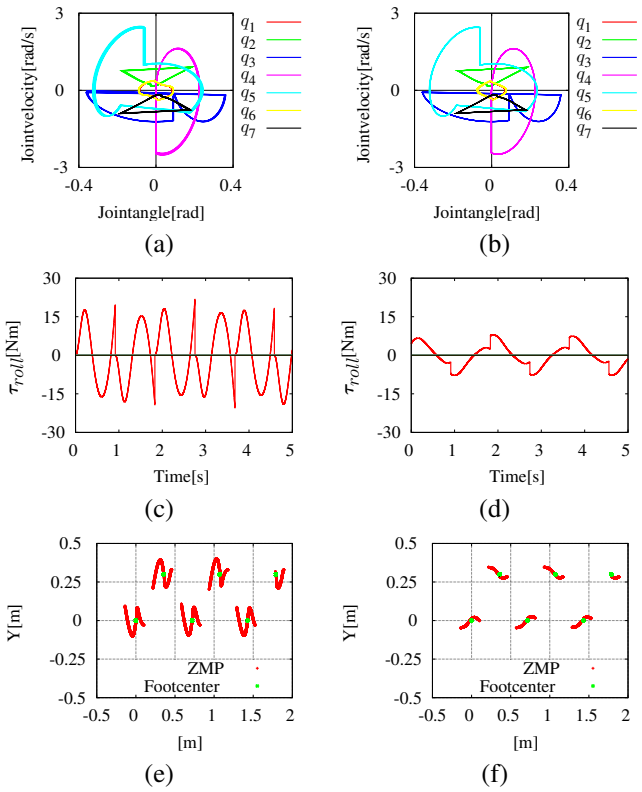

Fig. 7. Simulation results of limit cycle based walking of the 3D 7DOF biped model with two different desired trajectories for ankle roll: (a), (c) and (e) generated via a spline function; (b), (d) and (f) generated via an empirical reference trajectory. (a), (b) phase portrait, (c), (d) ankle roll control torque, (e), (f) center of the foot of the stance leg and ZMP paths.

of the motion in the frontal plane with the empirical roll reference trajectory.

VI. CONCLUSIONS

We think that the results presented in this paper are encouraging toward achieving our ultimate goal: energy-efficient walking pattern generation for a humanoid robot. We have shown that limit cycle based walking pattern generation is feasible for a relatively sophisticated 7DOF 3D biped robot, with mass distribution resembling that of a humanoid robot, and with flat feet as in present humanoid robots. The feasibility of the walking pattern has been also confirmed via ZMP analysis. Robustness could also be ensured by adopting an energy feedback control law. In addition, the calculation of the mechanical cost of transport has shown that our model is almost twice as efficient as that of a well known humanoid robot.

Based on these results, in our future work we plan to overcome systematically the remaining hurdles e.g. the design of the double stance phase, increasing the number of DOF's, a more rigorous approach to the generation of the ankle roll motion trajectory, appropriate foot link design and departing from the unnatural flat-foot approach, walk on uneven terrain along 3D paths etc. thus ensuring the implementation into a real humanoid.

REFERENCES

[1] S. Kajita and T. Sugihara, "Humanoid robots in the future," *J. of the Robotics Soc. of Japan*, vol. 26, no. 7, pp. 761–762, 2008 (in Japanese).

[2] S. Kajita, K. Yokoi, H. Hirukawa and K. Harada, "Biped walking," in *Humanoid Robot*, Tokyo, Japan: Ohmsha, 2005, pp. 103–161 (in Japanese).

[3] T. Sugihara and Y. Nakamura, "High mobility control of humanoid robots based on an analogy of ZMP-CoG model and carted inverted pendulum model," *J. of the Robotics Soc. of Japan*, vol. 24, no. 1, pp. 74–86, 2006 (in Japanese).

[4] D. N. Nenchev, Y. Tsumaki and A. Sekiguchi, "Motion feedback control at a singular configuration," *4th SICE System Integration Division Annu. Conf.*, Tokyo, Japan, 2003, pp. 508–509.

[5] Y. Ogura, T. Kataoka, K. Shimomura, H. Lim and A. Takanishi, "A novel method of biped walking pattern generation with predetermined knee joint motion," *in Proc. 2004 IEEE/RSJ Int. Conf. on Intelligent Robotics and Syst.*, Sendai, Japan, 2004, pp. 2381–2386.

[6] R. Kurazume, S. Tanaka, M. Yamashita and T. Hasegawa, "Straight legged walking of a biped robot," *in Proc. 2005 IEEE/RSJ Int. Conf. on Intelligent Robotics and Syst.*, Edmonton, Canada, 2005, pp. 3095–3101.

[7] K. Takahashi, M. Noda, D. N. Nenchev, Y. Tsumaki and A. Sekiguchi, "Static walk of a humanoid robot based on the singularity-consistent method," *in Proc. 2006 IEEE/RSJ Int. Conf. on Intelligent Robotics and Syst.*, Beijing, China, 2006, pp. 5484–5489.

[8] K. Kameta, A. Sekiguchi, Y. Tsumaki and Y. Kanamiya, "Walking control around singularity using a spherical inverted pendulum with an underfloor pivot," *in Proc. of 2007 IEEE-RAS Int. Conf. on Humanoid Robots)*, Pennsylvania, USA, 2007, Oral Paper Session SaP2 : Walking Control II.

[9] S. Mochon and T. A. McMahon, "Ballistic walking," *J. Biomechanics*, vol. 13, pp. 49–57, 1980.

[10] T. McGeer, "Passive dynamic walking," *The Int. J. of Robotics Research*, vol. 9, no. 2, pp. 62–82, 1990.

[11] S. H. Collins, A. Ruina, R. Tedrake and M. Wisse, "Efficient bipedal robots based on passive-dynamic walking," *Sci.*, vol. 307, pp. 1082–1085, 2005.

[12] A. Goswami, B. Espiau and A. Keramane, "Limit cycles in a passive compass gait biped and passivity-mimicking control laws," *Autonomous Robots*, vol. 4, no. 3, pp. 273–286, 1997.

[13] F. Asano, Z.W. Luo and M. Yamakita, "Some extensions of passive walking formula to active biped robots," *Proc. of the IEEE Int. Conf. Robotics and Automation*, New Orleans, LA, USA, 2004, pp. 3797-3802.

[14] T. McGeer, "Passive dynamic biped catalogue, 1991," in *Experimental Robotics II*, Toulouse, France: The 2nd Int. Symp., 1991, pp. 465–490.

[15] M. Wisse and A. L. Schwab, "Skateboards, bicycles, and 3D biped walking machines: A velocity dependent stability by means of lean-to-yaw coupling.," *The Int. J. of Robotics Research*, vol. 24, no. 6, pp. 417–429, 2005.

[16] S. H. Collins, M. Wisse and A. Ruina, "A three-dimensional passive-dynamic walking robot with two legs and knees," *The Int. J. of Robotics Research*, vol. 20, no. 7, pp. 607–615, 2001.

[17] M. Wisse, A. L. Schwab and R. Q. vd. Linde, "A 3D passive dynamic biped with yaw and roll compensation," *Robotica*, vol. 19, pp. 275–284, 2001.

[18] A. Kuo, "Stabilization of lateral motion in passive dynamic walking," *The Int. J. of Robotics Research*, vol. 18, no. 9, pp. 917–930, 1999.

[19] C. Chevallereau and J. W. Grizzle, "Asymptotically stable walking of a five-link underactuated 3-D bipedal robot," *IEEE Trans. Robotics*, vol. 25, no. 1, pp. 37–50, 2009.

[20] R. D. Gregg and M. W. Spong, "Bringing the compass-gait bipedal walker to three dimensions," *in Proc. 2009 IEEE/RSJ Int. Conf. on Intelligent Robotics and Syst.*, St. Louis, MO, USA, 2009, pp. 4469–4474.

[21] Y. Ikemata, K. Yasuhara, A. Sano and H. Fujimoto, "A study of the leg-swing motion of passive walking," *Proc. of the IEEE Int. Conf. Robotics and Automation*, Pasadena, CA, USA, 2008, pp. 1588–1593.

[22] K. Miyahara, Y. Harada, D. N. Nenchev and D. Sato, "Three-dimensional limit cycle walking with joint actuation," *in Proc. 2009 IEEE/RSJ Int. Conf. on Intelligent Robotics and Syst.*, St. Louis, MO, USA, 2009, pp. 4445–4450.

[23] F. Asano, Z. W. Luo, and M. Yamakita, "Biped gait generation and control based on a unified property of passive dynamic walking," *IEEE Trans. Robotics*, vol. 21, no. 4, pp. 754–762, 2005.